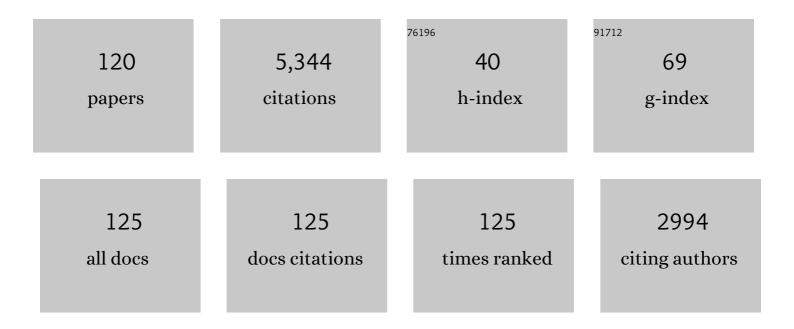
List of Publications by Year in descending order

Source: https://exaly.com/author-pdf/715528/publications.pdf Version: 2024-02-01



ΠΑΎΕ ΕΛΤΟΝ

#	Article	IF	CITATIONS
1	Fault activation by hydraulic fracturing in western Canada. Science, 2016, 354, 1406-1409.	6.0	400
2	The elusive lithosphere–asthenosphere boundary (LAB) beneath cratons. Lithos, 2009, 109, 1-22.	0.6	365
3	Hydraulic Fracturing and Seismicity in the Western Canada Sedimentary Basin. Seismological Research Letters, 2016, 87, 631-647.	0.8	329
4	Two crustal low-velocity channels beneath SE Tibet revealed by joint inversion of Rayleigh wave dispersion and receiver functions. Earth and Planetary Science Letters, 2015, 415, 16-24.	1.8	229
5	Hydraulic Fracturingâ€Induced Seismicity. Reviews of Geophysics, 2020, 58, e2019RC000695.	9.0	202
6	Hydraulic fracturing volume is associated with induced earthquake productivity in the Duvernay play. Science, 2018, 359, 304-308.	6.0	181
7	The role of aseismic slip in hydraulic fracturing–induced seismicity. Science Advances, 2019, 5, eaav7172.	4.7	173
8	A review and appraisal of arrival-time picking methods for downhole microseismic data. Geophysics, 2016, 81, KS71-KS91.	1.4	145
9	Developments in understanding seismicity triggered by hydraulic fracturing. Nature Reviews Earth & Environment, 2020, 1, 264-277.	12.2	123
10	Spatiotemporal variations in the b-value of earthquake magnitude–frequency distributions: Classification and causes. Tectonophysics, 2014, 615-616, 1-11.	0.9	118
11	Discriminating induced seismicity from natural earthquakes using moment tensors and source spectra. Journal of Geophysical Research: Solid Earth, 2016, 121, 972-993.	1.4	90
12	Velocity–conductivity relationships for mantle mineral assemblages in Archean cratonic lithosphere based on a review of laboratory data and Hashin–Shtrikman extremal bounds. Lithos, 2009, 109, 131-143.	0.6	89
13	Induced Seismicity Characterization during Hydraulicâ€Fracture Monitoring with a Shallowâ€Wellbore Geophone Array and Broadband Sensors. Seismological Research Letters, 2018, 89, 1641-1651.	0.8	89
14	Seismic evidence for convection-driven motion of the North American plate. Nature, 2007, 446, 428-431.	13.7	87
15	Plateau uplift in western Canada caused by lithospheric delamination along a craton edge. Nature Geoscience, 2014, 7, 830-833.	5.4	86
16	Solid angles and the impact of receiver-array geometry on microseismic moment-tensor inversion. Geophysics, 2011, 76, WC77-WC85.	1.4	83
17	Increased likelihood of induced seismicity in highly overpressured shale formations. Geophysical Journal International, 2018, 214, 751-757.	1.0	82
18	Tectonic entrapment and its role in the evolution of continental lithosphere: An example from the Precambrian of western Canada. Tectonics, 2000, 19, 116-134.	1.3	76

DAVE EATON

#	Article	IF	CITATIONS
19	Microseismic Monitoring Developments in Hydraulic Fracture Stimulation. , 0, , .		76
20	Formation of cratonic mantle keels by arc accretion: Evidence from S receiver functions. Geophysical Research Letters, 2010, 37, .	1.5	74
21	New insights into the lithosphere beneath the Superior Province from Rayleigh wave dispersion and receiver function analysis. Geophysical Journal International, 2007, 169, 1043-1068.	1.0	71
22	Episodic Lithospheric Deformation in Eastern Tibet Inferred From Seismic Anisotropy. Geophysical Research Letters, 2020, 47, e2019GL085721.	1.5	69
23	Paleoproterozoic collisional orogen beneath the western Canada sedimentary basin imaged by Lithoprobe crustal seismic-reflection data. Geology, 1995, 23, 195.	2.0	65
24	Crustal thickness and VP/VS variations in the Grenville orogen (Ontario, Canada) from analysis of teleseismic receiver functions. Tectonophysics, 2006, 420, 223-238.	0.9	63
25	Seismic imaging of the lithosphere beneath Hudson Bay: Episodic growth of the Laurentian mantle keel. Earth and Planetary Science Letters, 2013, 373, 179-193.	1.8	61
26	The Cardston Earthquake Swarm and Hydraulic Fracturing of the Exshaw Formation (Alberta Bakken) Tj ETQq0 0	0 rgBT /O	verlock 10 Tf
27	Magnetotelluric and teleseismic study across the Snowbird Tectonic Zone, Canadian Shield: A Neoarchean mantle suture?. Geophysical Research Letters, 2002, 29, 10-1-10-4.	1.5	59
28	Enhanced Geothermal Systems (EGS): Hydraulic fracturing in a thermo-poroelastic framework. Journal of Petroleum Science and Engineering, 2016, 146, 1179-1191.	2.1	59
29	Scaling relations and spectral characteristics of tensile microseisms: evidence for opening/closing cracks during hydraulic fracturing. Geophysical Journal International, 2014, 196, 1844-1857.	1.0	58
30	Breakdown of the Gutenbergâ€Richter relation for microearthquakes induced by hydraulic fracturing: influence of stratabound fractures. Geophysical Prospecting, 2014, 62, 806-818.	1.0	57
31	Multi-genetic origin of the continental Moho: insights from Lithoprobe. Terra Nova, 2006, 18, 34-43.	0.9	55
32	Lithospheric variations across the Superior Province, Ontario, Canada: Evidence from tomography and shear wave splitting. Journal of Geophysical Research, 2007, 112, .	3.3	55
33	Sourceâ€Mechanism Analysis and Stress Inversion for Hydraulicâ€Fracturingâ€Induced Event Sequences near Fox Creek, Alberta. Bulletin of the Seismological Society of America, 2019, 109, 636-651.	1.1	55
34	Joint inversion of teleseismic receiver functions and magnetotelluric data using a genetic algorithm: Are seismic velocities and electrical conductivities compatible?. Geophysical Research Letters, 2007, 34,	1.5	54

35	Microseismicity reveals fault activation before Mw 4.1 hydraulic-fracturing induced earthquake. Geophysical Journal International, 2019, 218, 534-546.	1.0	50
36	Lithospheric architecture and tectonic evolution of the Hudson Bay region. Tectonophysics, 2010, 480, 1-22.	0.9	49

3

•

#	Article	IF	CITATIONS
37	Seismic-reflection and potential-field studies of the Vulcan structure, western Canada: A Paleoproterozoic Pyrenees?. Journal of Geophysical Research, 1999, 104, 23255-23269.	3.3	46
38	Lithospheric anisotropy structure inferred from collocated teleseismic and magnetotelluric observations: Great Slave Lake shear zone, northern Canada. Geophysical Research Letters, 2004, 31, .	1.5	46
39	Crustal structure beneath Hudson Bay from ambient-noise tomography: implications for basin formation. Geophysical Journal International, 2011, 184, 65-82.	1.0	46
40	Precambrian plate tectonics: Seismic evidence from northern Hudson Bay, Canada. Geology, 2011, 39, 91-94.	2.0	43
41	Stress and fault parameters affecting fault slip magnitude and activation time during a glacial cycle. Tectonics, 2014, 33, 1461-1476.	1.3	43
42	Large‣cale Fracture Systems Are Permeable Pathways for Fault Activation During Hydraulic Fracturing. Journal of Geophysical Research: Solid Earth, 2021, 126, e2020JB020311.	1.4	40
43	Proterozoic tectonic accretion and growth of western Laurentia: results from Lithoprobe studies in northern Alberta. Canadian Journal of Earth Sciences, 2002, 39, 313-329.	0.6	38
44	What controls the maximum magnitude of injection-induced earthquakes?. The Leading Edge, 2018, 37, 135-140.	0.4	38
45	Focal Mechanisms of Some Inferred Induced Earthquakes in Alberta, Canada. Seismological Research Letters, 2015, 86, 1078-1085.	0.8	37
46	Ephemeral isopycnicity of cratonic mantle keels. Nature Geoscience, 2013, 6, 967-970.	5.4	36
47	LITHOPROBE reflection studies of Archean and Proterozoic crust in Canada. Tectonophysics, 1996, 264, 65-88.	0.9	35
48	The lithospheric root beneath Hudson Bay, Canada from Rayleigh wave dispersion: No clear seismological distinction between Archean and Proterozoic mantle. Lithos, 2010, 120, 144-159.	0.6	33
49	Bilinear Magnitudeâ€Frequency Distributions and Characteristic Earthquakes During Hydraulic Fracturing. Geophysical Research Letters, 2018, 45, 12,866.	1.5	32
50	Crustal structure beneath the Western Canada Sedimentary Basin: constraints from gravity and magnetic modelling. Canadian Journal of Earth Sciences, 2002, 39, 291-312.	0.6	31
51	Crustal anisotropy beneath Hudson Bay from ambient noise tomography: Evidence for postâ€orogenic lowerâ€crustal flow?. Journal of Geophysical Research, 2012, 117, .	3.3	31
52	A Long-Lived Swarm of Hydraulic Fracturing-Induced Seismicity Provides Evidence for Aseismic Slip. Bulletin of the Seismological Society of America, 2020, 110, 2205-2215.	1.1	31
53	Machine Learningâ€Based Analysis of Geological Susceptibility to Induced Seismicity in the Montney Formation, Canada. Geophysical Research Letters, 2020, 47, e2020GL089651.	1.5	31
54	Moment tensors, state of stress and their relation to post-glacial rebound in northeastern Canada. Geophysical Journal International, 2012, 189, 1741-1752.	1.0	27

#	Article	IF	CITATIONS
55	Comparing Energy Calculations - Hydraulic Fracturing and Microseismic Monitoring. , 2012, , .		27
56	InSAR data reveal that the largest hydraulic fracturing-induced earthquake in Canada, to date, is a slow-slip event. Scientific Reports, 2022, 12, 2043.	1.6	26
57	Nontrivial clustering of microseismicity induced by hydraulic fracturing. Geophysical Research Letters, 2016, 43, 10,672.	1.5	22
58	Inversion and interpretation of seismic-derived rock properties in the Duvernay play. Interpretation, 2018, 6, SE1-SE14.	0.5	22
59	2b or not 2b? Interpreting magnitude distributions from microseismic catalogs. First Break, 2015, 33, .	0.2	22
60	Structure of the crust and upper mantle of the Great Slave Lake shear zone, northwestern Canada, from teleseismic analysis and gravity modelling. Canadian Journal of Earth Sciences, 2003, 40, 1203-1218.	0.6	21
61	Quantifying Fracture Networks Inferred From Microseismic Point Clouds by a Gaussian Mixture Model With Physical Constraints. Geophysical Research Letters, 2019, 46, 11008-11017.	1.5	21
62	Detection and analysis of microseismic events using a Matched Filtering Algorithm (MFA). Geophysical Journal International, 0, , ggw168.	1.0	19
63	Interevent Triggering in Microseismicity Induced by Hydraulic Fracturing. Bulletin of the Seismological Society of America, 2018, 108, 1133-1146.	1.1	19
64	Passive Seismic Monitoring and Integrated Geomechanical Analysis of a Tight-Sand Reservoir During Hydraulic-Fracture Treatment, Flowback and Production. , 2014, , .		18
65	The Hudson Bay Lithospheric Experiment (HuBLE): insights into Precambrian plate tectonics and the development of mantle keels. Geological Society Special Publication, 2015, 389, 41-67.	0.8	18
66	Large variations in lithospheric thickness of western Laurentia: Tectonic inheritance or collisional reworking?. Precambrian Research, 2015, 266, 579-586.	1.2	17
67	Rayleigh wave azimuthally anisotropic phase velocity maps beneath western Canada. Journal of Geophysical Research: Solid Earth, 2016, 121, 1821-1834.	1.4	17
68	Anatomy of a buried thrust belt activated during hydraulic fracturing. Tectonophysics, 2020, 795, 228640.	0.9	17
69	Focal-time analysis: A new method for stratigraphic depth control of microseismicity and induced seismic events. Geophysics, 2019, 84, KS173-KS182.	1.4	16
70	Refinement of arrival-time picks using a cross-correlation based workflow. Journal of Applied Geophysics, 2016, 135, 55-66.	0.9	14
71	Application of structural interpretation and simultaneous inversion to reservoir characterization of the Duvernay Formation, Fox Creek, Alberta, Canada. The Leading Edge, 2019, 38, 151-160.	0.4	14
72	Hydro-mechanically coupled FDEM framework to investigate near–wellbore hydraulic fracturing in homogeneous and fractured rock formations. Journal of Petroleum Science and Engineering, 2017, 154, 100-113.	2.1	13

#	Article	IF	CITATIONS
73	Seismicity‣canning Based on Navigated Automatic Phaseâ€Picking. Journal of Geophysical Research: Solid Earth, 2019, 124, 3802-3818.	1.4	12
74	Energy-based hydraulic fracture numerical simulation: Parameter selection and model validation using microseismicity. Geophysics, 2015, 80, W33-W44.	1.4	11
75	The Application of Coda and Energy Methods for Magnitude Estimation of Microseismic Events. Seismological Research Letters, 2019, 90, 1296-1307.	0.8	11
76	Unprecedented quiescence in resource development area allows detection of long-lived latent seismicity. Solid Earth, 2021, 12, 765-783.	1.2	10
77	Seismic hazard due to fluid injections. Physical Review Research, 2020, 2, .	1.3	10
78	Reservoir characterization using microseismic facies analysis integrated with surface seismic attributes. Interpretation, 2016, 4, T167-T181.	0.5	9
79	Automated Microseismic Processing and Integrated Interpretation of Induced Seismicity during a Multistage Hydraulic-Fracturing Stimulation, Alberta, Canada. Bulletin of the Seismological Society of America, 2020, 110, 2018-2030.	1.1	9
80	Historical seismicity of the Jordan Dead Sea Transform region and seismotectonic implications. Arabian Journal of Geosciences, 2015, 8, 4039-4055.	0.6	8
81	Determination of stimulated reservoir volume and anisotropic permeability using analytical modelling of microseismic and hydraulic fracturing parameters. Journal of Natural Gas Science and Engineering, 2018, 58, 234-240.	2.1	8
82	Integration of outcrop, subsurface, and microseismic interpretation for rock-mass characterization: An example from the Duvernay Formation, Western Canada. Interpretation, 2018, 6, T919-T936.	0.5	8
83	The Influence of a Transitional Stress Regime on the Source Characteristics of Induced Seismicity and Fault Activation: Evidence from the 30 November 2018 Fort St. John ML 4.5 Induced Earthquake Sequence. Bulletin of the Seismological Society of America, 2022, 112, 1336-1355.	1.1	8
84	A <i>k</i> -mean characteristic function for optimizing short- and long-term-average-ratio-based detection of microseismic events. Geophysics, 2019, 84, KS143-KS153.	1.4	7
85	Intraplate seismicity in Canada: a graph theoretic approach to data analysis and interpretation. Nonlinear Processes in Geophysics, 2010, 17, 513-527.	0.6	6
86	Moho Structure Across the Backarcâ€Craton Transition in the Northern U.S. Cordillera. Tectonics, 2020, 39, e2019TC005489.	1.3	6
87	Integrated approach for fracture characterization of hydraulically stimulated volume in tight gas reservoir. Journal of Petroleum Exploration and Production, 2019, 9, 2429-2440.	1.2	5
88	Vertical and lateral facies variability in organic-rich mudstones at the reservoir scale: A case study from the Devonian Duvernay formation of Alberta, Canada. Marine and Petroleum Geology, 2021, 132, 105232.	1.5	5
89	The interplay between cm- and m-scale geological and geomechanical heterogeneity in organic-rich mudstones: Implications for reservoir characterization of unconventional shale plays. Journal of Natural Gas Science and Engineering, 2022, 97, 104363.	2.1	5
90	Fully coupled hydro–mechanical controls on non-diffusive seismicity triggering front driven by hydraulic fracturing. Journal of Seismology, 2019, 23, 109-121.	0.6	4

#	Article	IF	CITATIONS
91	Determining elastic properties of organic-rich shales from core, wireline logs and 3-D seismic: A comparative study from the Duvernay play, Alberta, Canada. Journal of Natural Gas Science and Engineering, 2020, 84, 103637.	2.1	4
92	Seismic Anisotropy Reveals Stress Changes around a Fault as It Is Activated by Hydraulic Fracturing. Seismological Research Letters, 2022, 93, 1737-1752.	0.8	4
93	Introduction to special section: Low-permeability resource plays of the Western Canada Sedimentary Basin — Defining the sweet spots. Interpretation, 2018, 6, SEi-SEii.	0.5	3
94	A regularized approach for estimation of a composite focal mechanism from a set of microearthquakes. Geophysics, 2018, 83, KS65-KS75.	1.4	3
95	Application of focal-time analysis for improved induced seismicity depth control: A case study from the Montney Formation, British Columbia, Canada. Geophysics, 2020, 85, KS185-KS196.	1.4	3
96	Characterization of damage processes in Montney siltstone under triaxial compression using acoustic emission and diagnostic imaging. Geophysical Journal International, 2021, 228, 2005-2017.	1.0	3
97	Spatiotemporal Clustering of Seismicity in the Kiskatinaw Seismic Monitoring and Mitigation Area. Frontiers in Earth Science, 2022, 10, .	0.8	3
98	Basement Tectonics and Fault Reactivation in Alberta Based on Seismic and Potential Field Data. , 0, , .		2
99	Ground-Motion Analysis of Hydraulic-Fracturing Induced Seismicity at Close Epicentral Distance. Bulletin of the Seismological Society of America, 2020, 110, 331-344.	1.1	2
100	Static Ground Displacement for an Induced Earthquake Recorded on Broadband Seismometers. Bulletin of the Seismological Society of America, 2020, 110, 2216-2224.	1.1	2
101	Realâ€Time Earthquake Location Based on the Kalman Filter Formulation. Geophysical Research Letters, 2020, 47, e2019GL086240.	1.5	2
102	Fluid flow and thermal modeling for tracking induced seismicity near the Graham disposal well, British Columbia, Canada. , 2018, , .		2
103	Further insights on the role of aseismic slip in hydraulic fracturing-induced seismicity. , 2020, , .		2
104	Integrated interpretation: Defining risk corridors by combining 3-D seismic interpretation with induced seismicity hypocenters. Tectonophysics, 2022, 827, 229263.	0.9	2
105	Path effects in subsurface microseismic monitoring. The Leading Edge, 2012, 31, 1326-1329.	0.4	1
106	Induced Seismicity Near Fox Creek, Alberta: Interpretation of Source Mechanisms. , 2018, , .		1
107	Examining Hydraulic Fracture Characteristics Based on Induced Microseismicity: A Barnett Shale Case Study. , 2019, , .		1
108	A Novel Equivalent Continuum Approach for Modelling Hydraulic Fractures. Energies, 2020, 13, 6187.	1.6	1

#	Article	IF	CITATIONS
109	Geomechanical and Fracture Network Interpretation of a Devonian Outcrop. SPE Reservoir Evaluation and Engineering, 2021, 24, 692-707.	1.1	1
110	The influence of competing regional stress regimes on the generation of hydraulic fracturing-induced microseismicity. , 2020, , .		1
111	Persistent postinjection induced seismicity near Fox Creek, Alberta. , 2018, , .		1
112	Automated mapping of hydraulic fractures using bedding-plane slip events. , 2019, , .		1
113	Induced seismicity risk analysis using a novel 3D modelling approach. , 2021, , .		0
114	Change in microseismic anisotropy lag time reveals stress changes around a fault. , 2021, , .		0
115	Focal-time estimation: A new method for stratigraphic depth control of induced seismicity. , 2018, , .		0
116	Moment tensor and stress inversion based on hydraulic-fracturing induced events. , 2018, , .		0
117	Synthetic modelling to recognize potential duplex waves from basement faults in western Canada. , 2019, , .		0
118	Energy-stack: a fast and robust method for real-time microseismic event-detection. Technical Papers Rio Oil & Gas, 2020, 20, 3-4.	0.0	0
119	Integrated interpretation: Using seismic data to de-risk development of the Duvernay Formation, western Canada. , 2020, , .		0
120	Evidence for Postâ€Assembly Modification of Western Laurentia by Backâ€Arc Extension. Tectonics, 2022, 41, .	1.3	0